New Carbon Materials, 2024, 39(1): 142-151

A Co_3O_4/graphdiyne heterointerface for efficient ammonia production from nitrates

Zhao-yang Chen, Shu-ya Zhao, Xiao-yu Luan, Zhi-qiang Zheng, Jia-yu Yan, Yu-rui Xue*

Shandong Provincial Key Laboratory for Science of Material Creation and Energy Conversion, Science Center for Material Creation and Energy Conversion, School of Chemistry and Chemical Engineering, Shandong University, Jinan 250100, China

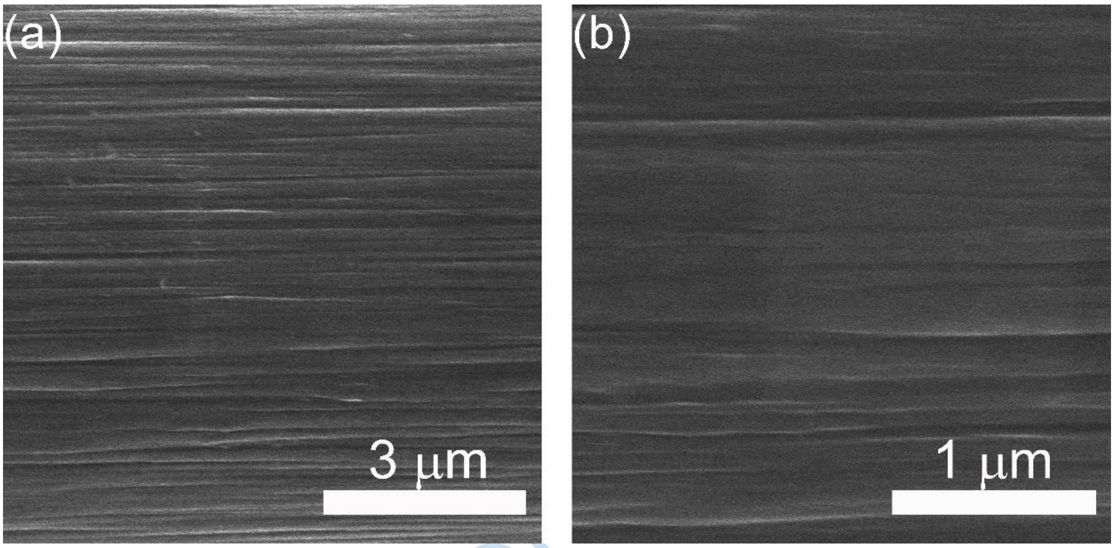

Fig. S1 (a) Low- and (b) high-magnification SEM images of the CC.

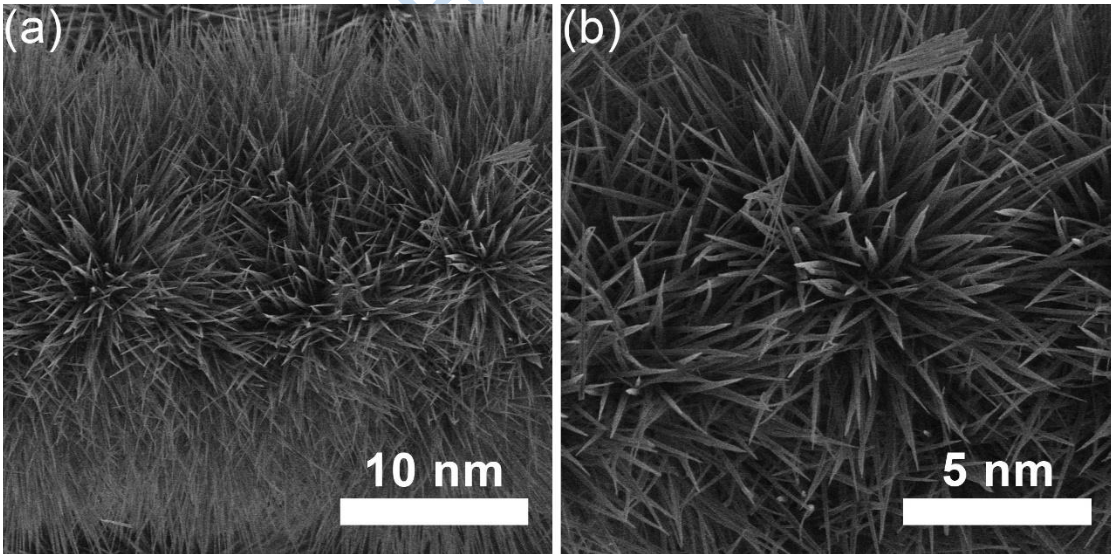

Fig. S2 (a) Low- and (b) high-magnification SEM images of the Co precursor.

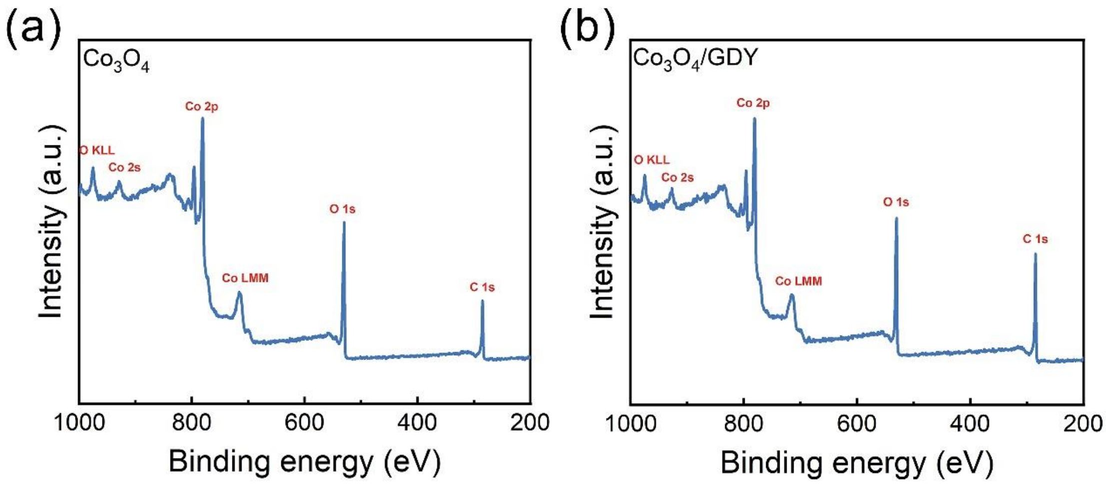

Fig. S3 (a) XPS survey of Co_3O_4. (b) XPS survey of Co_3O_4/GDY.

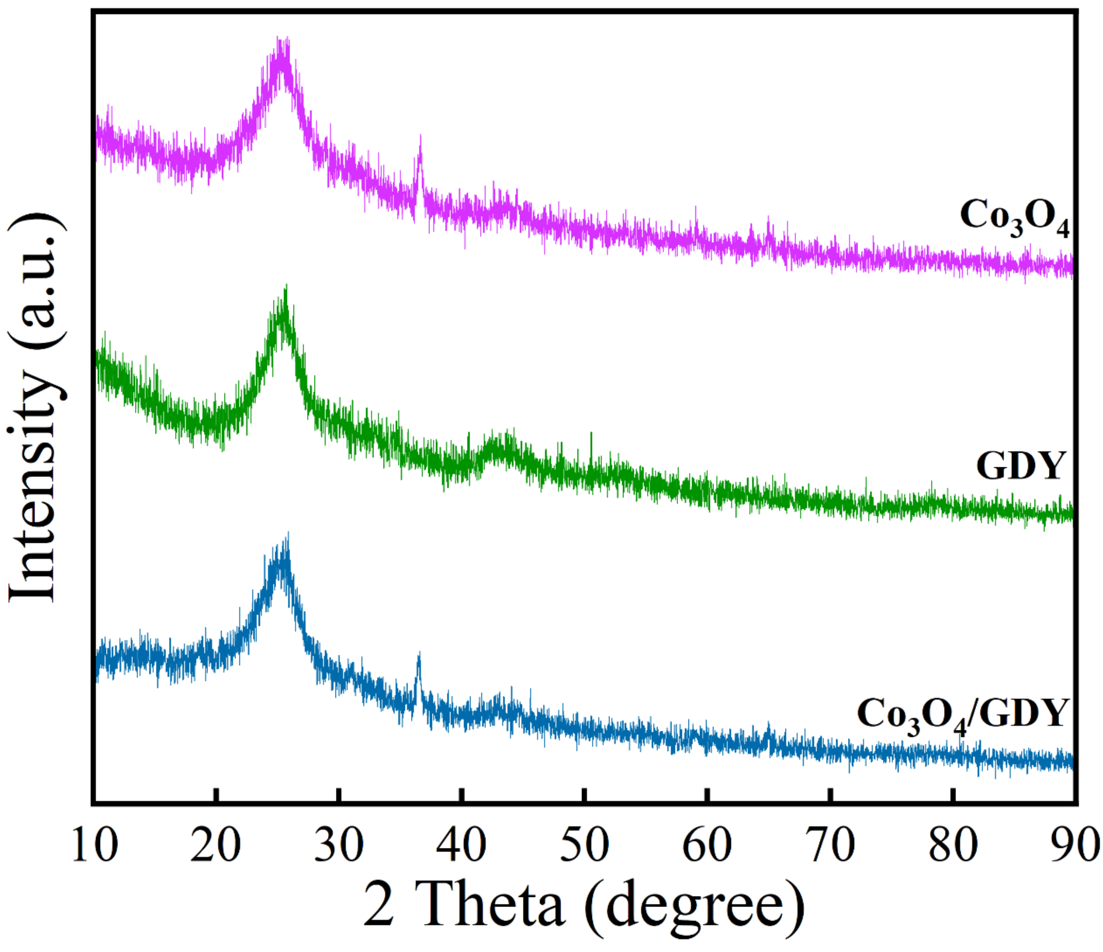

Fig. S4 Comparison of XRD patterns.

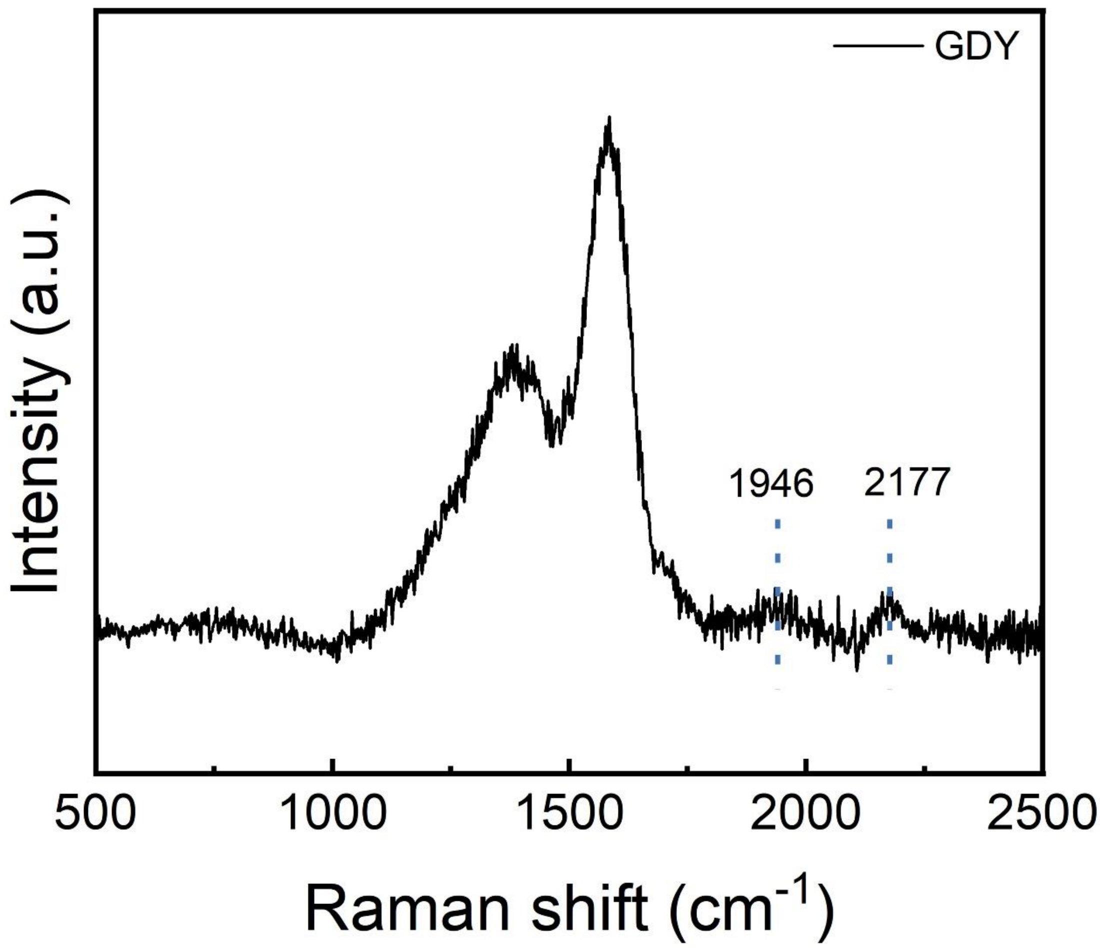

Fig. S5 Raman spectra of GDY.

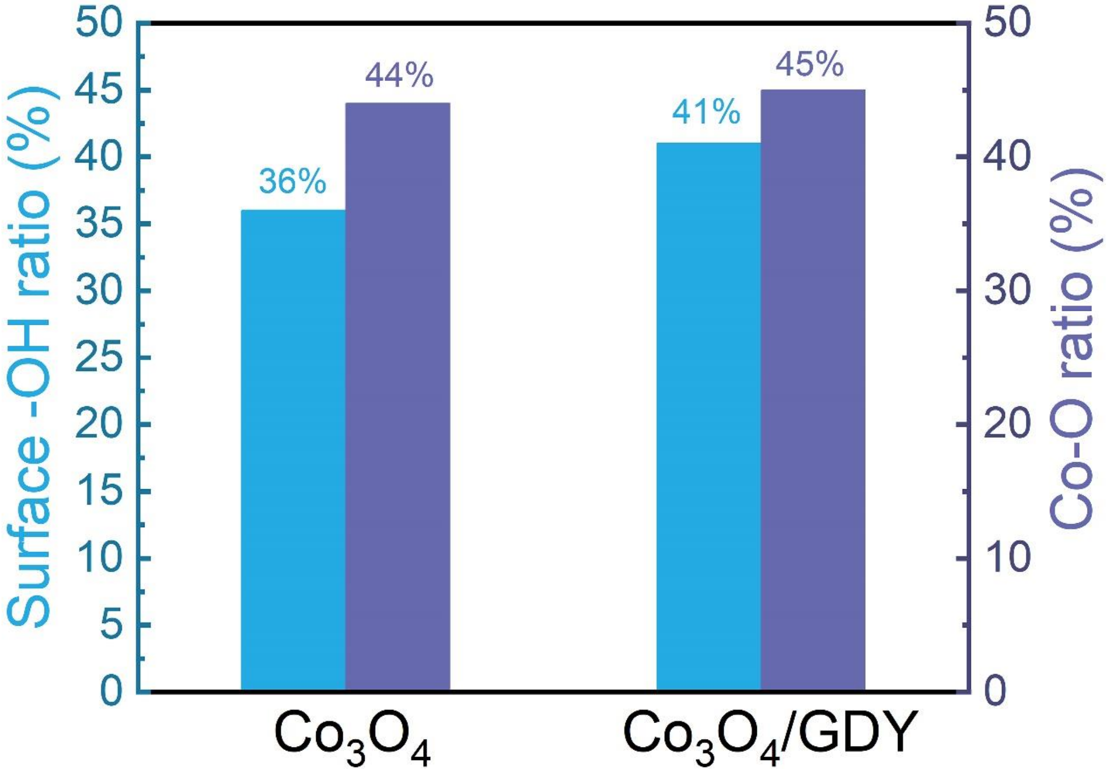

Fig. S6 Comparison of surface -OH ratio and Co-O ratio between Co_3O_4 and Co_3O_4/GDY.

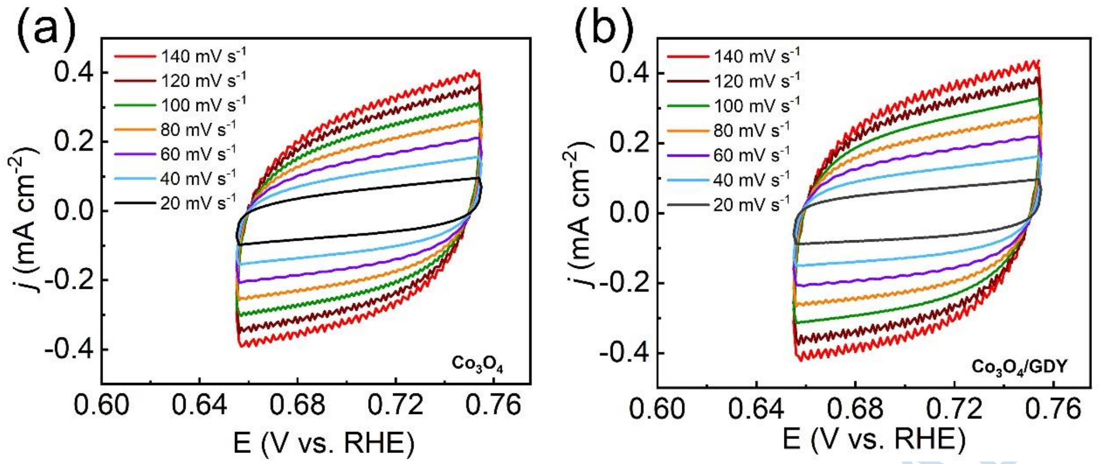

Fig. S7 Cyclic voltammograms test for (a) Co_3O_4, and (b) Co_3O_4/GDY at different scan rates from 20 to 140 mV s^{-1}.

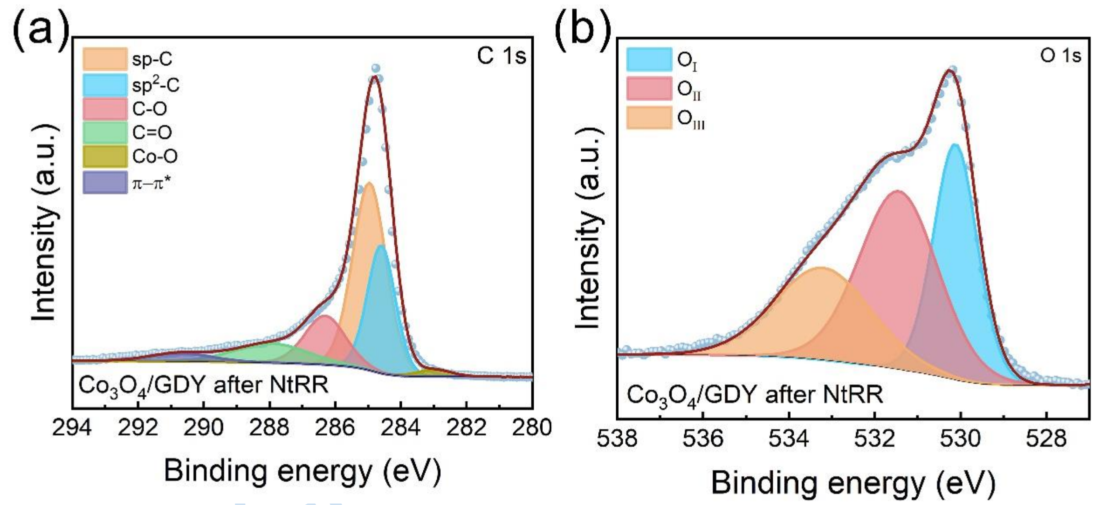

Fig. S8 (a) C 1s XPS spectra of Co_3O_4/GDY after NtRR. (b) O 1s XPS spectra of Co_3O_4/GDY after NtRR.

C

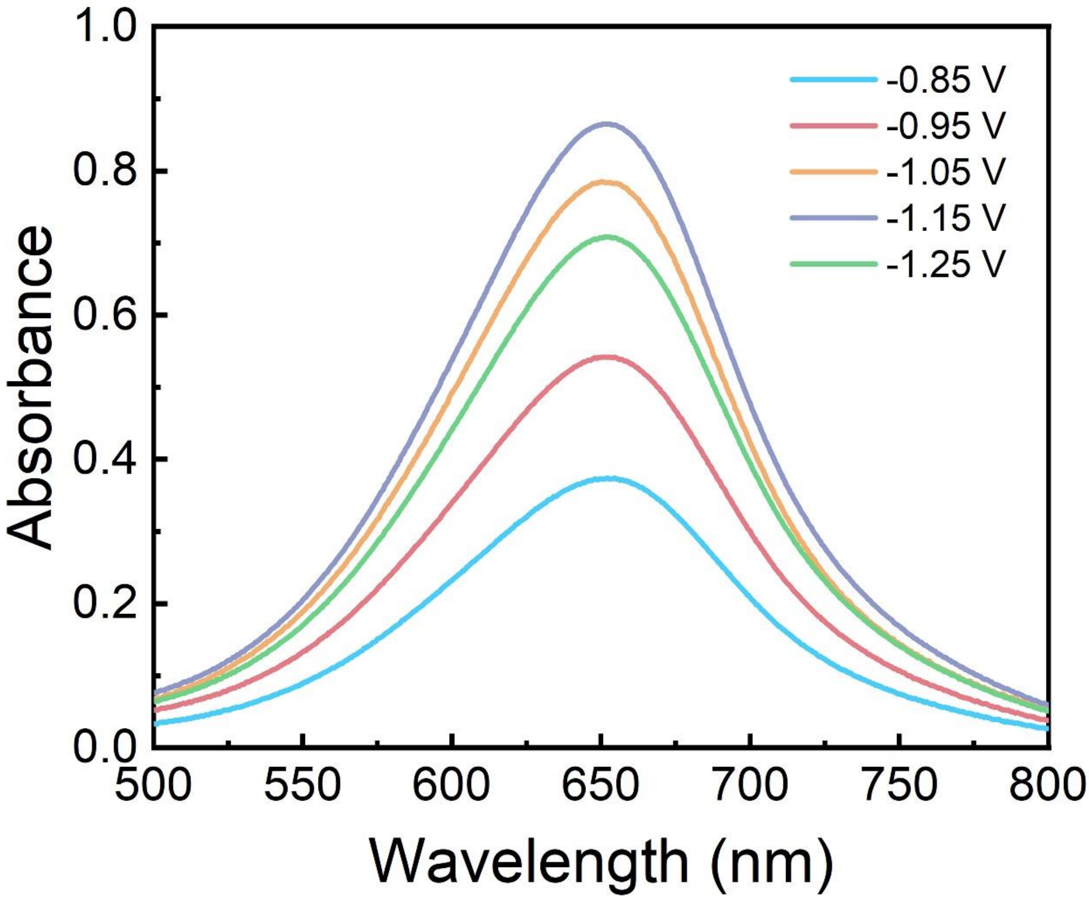

Fig. S9 Absorbance of Co_3O_4/GDY at different potentials in 0.5 M K_2SO_4 + 0.1 M NO_3^-. The solutions were diluted for 25 times.

C

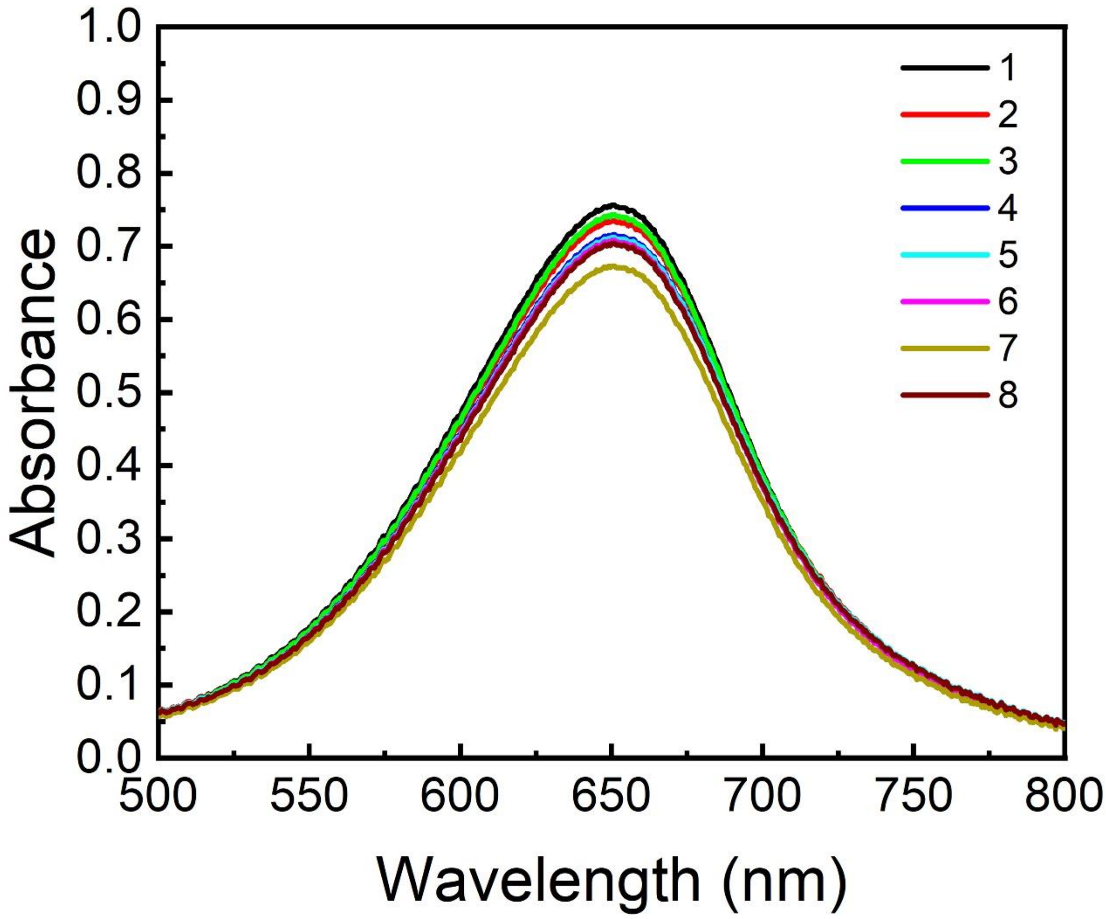

Fig. S10. Stability test of Co_3O_4/GDY at -1.05 V (vs RHE).

C

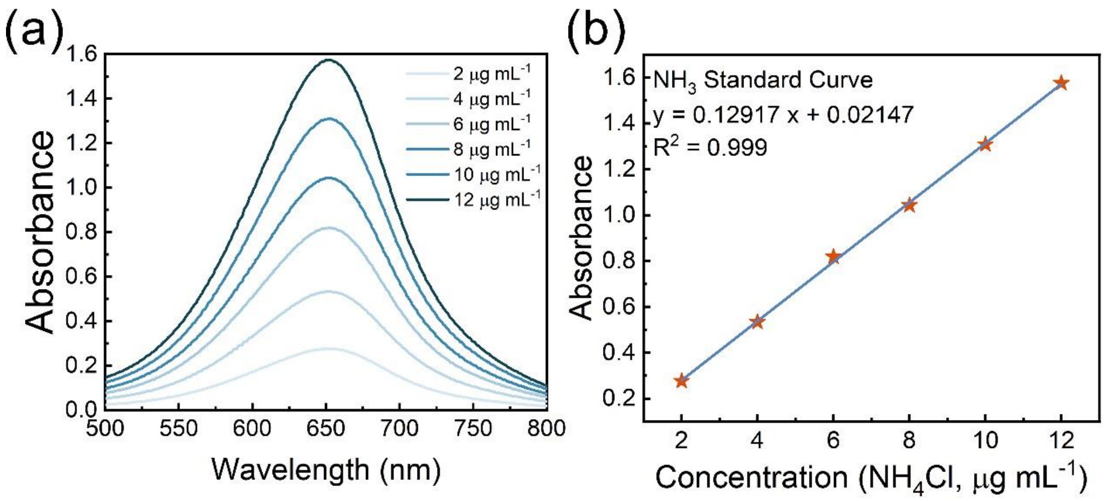

Fig. S11 Calibration curves for NH_4^+ determination. (a) Absorption spectra of the solutions containing NH_4Cl at different NH_4Cl concentrations. (b) A linear relationship between the absorbance at 652.5 nm and the NH_4Cl concentration.

C

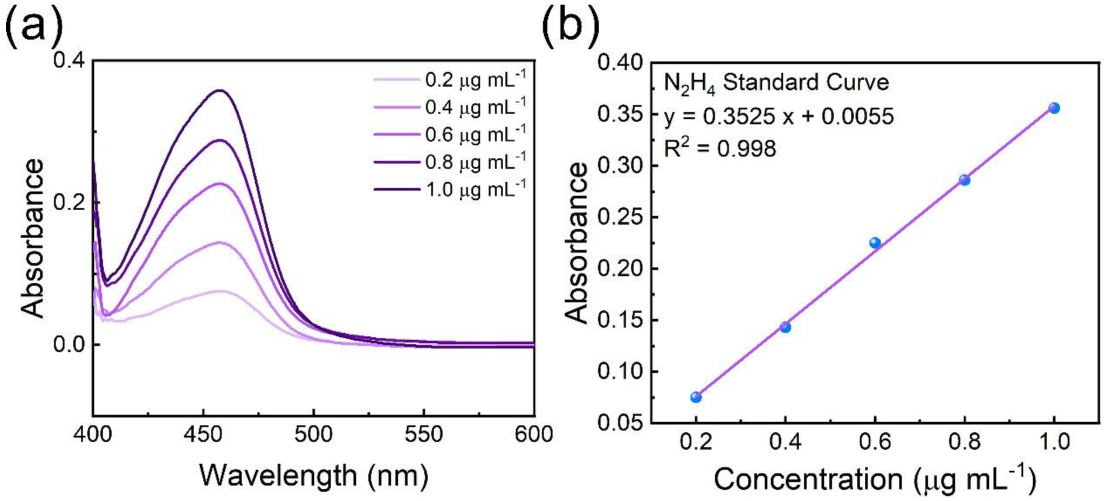

Fig. S12. Calibration curves for N_2H_4 determination. (a) Absorption spectra of the solutions containing N_2H_4 at different N_2H_4 concentrations. (b) A linear relationship between the absorbance at 455 nm and the N_2H_4 concentration.

C

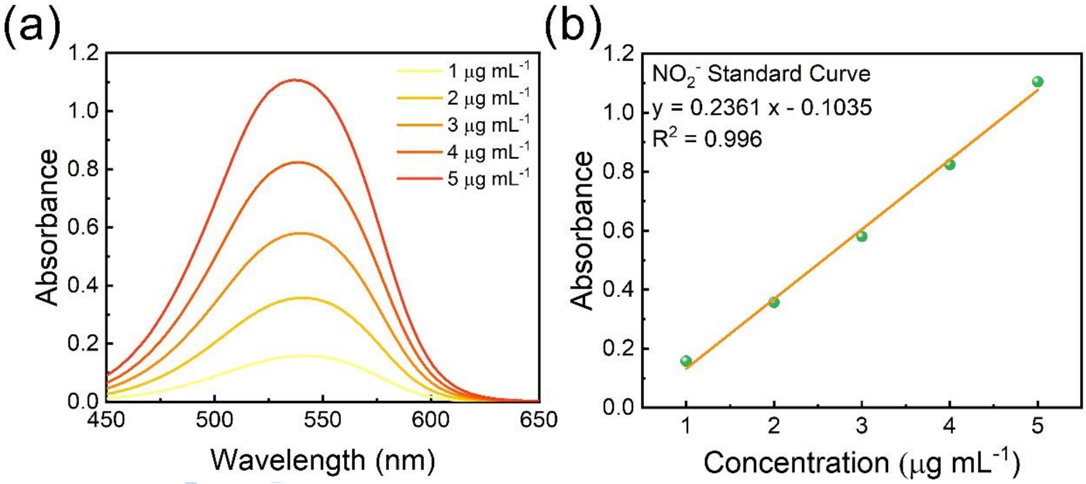

Fig. S13. Calibration curves for NO_2^- determination. (a) Absorption spectra of the solutions containing KNO_2 at different KNO_2 concentrations. (b) A linear relationship between the absorbance at 540 nm and the KNO_2 concentration.

C

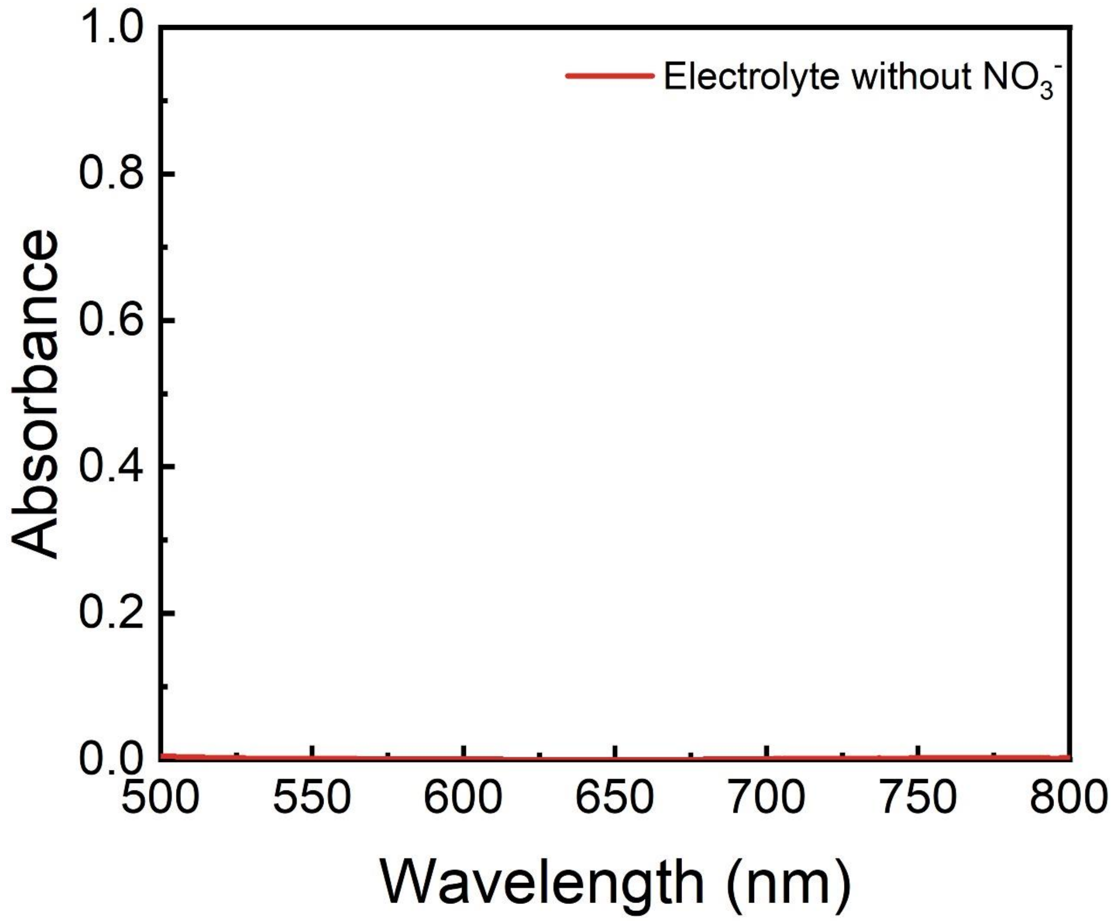

Fig. S14. Absorption spectra of the solutions without NO_3^- after NtRR of Co_3O_4/GDY.

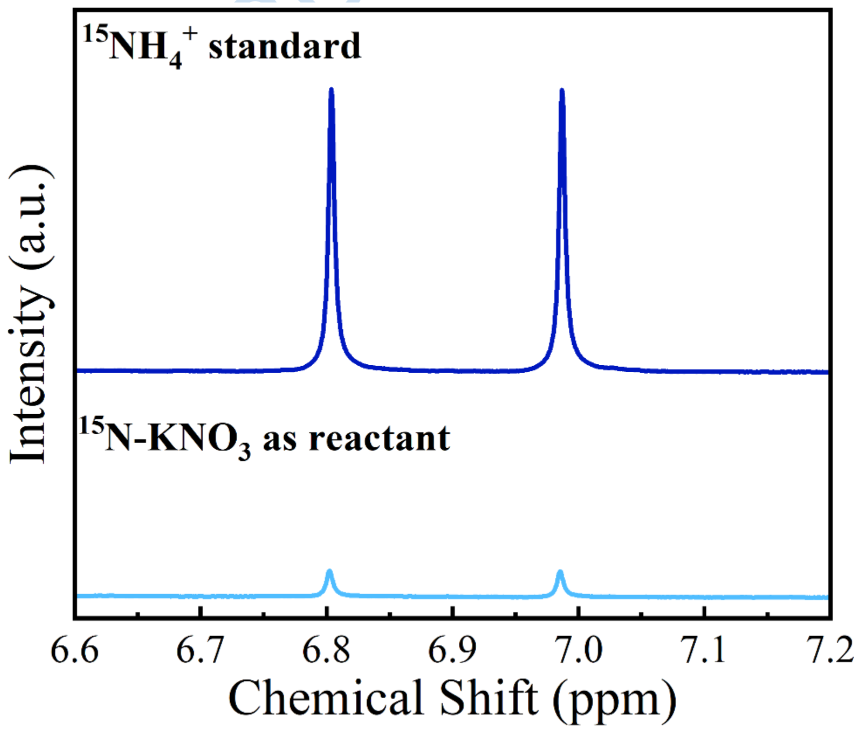

Fig. S15. ^{1}H-NMR spectra of the electrolytes obtained after NtRR for 0.5 h using $^{15}NO_3^-$ as the nitrogen sources.

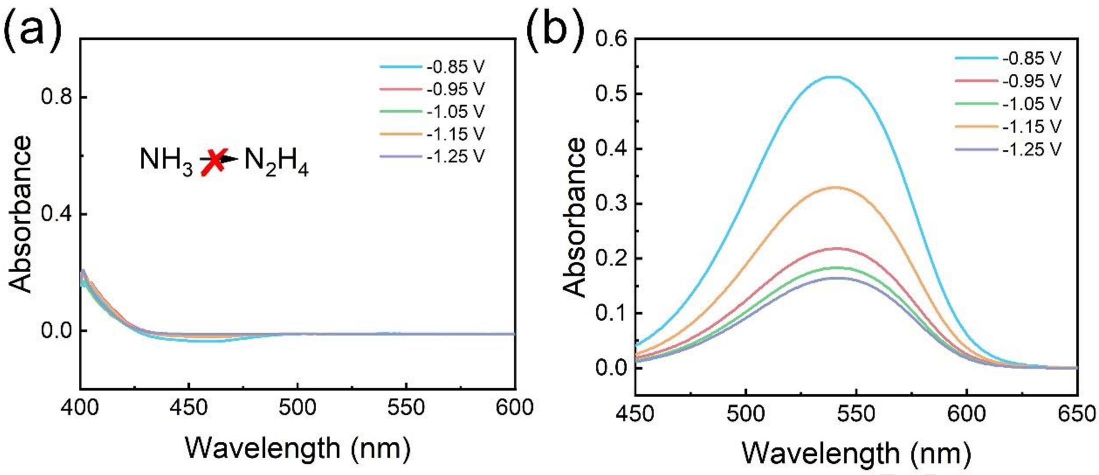

Fig. S16. Absorption spectra of the solutions containing (a) N_2H_4. (b) NO_2^- after NtRR of Co_3O_4/GDY at different potentials.

Table S1. Comparison of NtRR performance between Co_3O_4/GDY and recently reported electrocatalysts.

Electrocatalyst	Electrolyte	Y_{NH3}	FE (%)	Reference
Co_3O_4/GDY	0.5 M K_2SO_4 + 0.1 M KNO_3	0.79 mmol h^{-1} cm^{-2}	92.45	This work
PP-Co	0.1 M NaOH + 0.1 M NO_3^-	1.1 mmol h^{-1} $mg_{cat.}^{-1}$	90.1	[1]
Cu_{SA}NPC	0.01 M PBS + 500 mg L^{-1} NO_3^--N	2602μg h^{-1} cm^{-2}	87.2	[2]
Fe SAC	0.1 M K_2SO_4 + 0.5 M KNO_3	20000μg h^{-1} $mg_{cat.}^{-1}$	75	[3]
$Ni_3Co_6S_8$	1 M KOH + 20-1000 mg L^{-1} NO_3^--N	2388.4μg h^{-1} cm^{-2}	85.3	[4]
Mn_3O_4/CuOx	0.5 M Na_2SO_4 + 200 ppm NO_3^--N	0.1780 mmol h^{-1} cm^{-2}	86.55	[5]
FeCo PBA HCAs	0.1 M PBS + 0.1 M NaNO3	1788.4μg h^{-1} cm^{-2}	81.01	[6]
Fe/Cu-HNG	0.1 M KOH + 0.1 M KNO_3	1.08 mmol h^{-1} mg^{-1}	92.51	[7]
Ru@C_3N_4/Cu	0.5 M Na_2SO_4 + 200 ppm NO_3^--N	0.249 mmol h^{-1} cm^{-2}	91.3	[8]
FeOOH/CP	0.1 M PBS + 0.1 M NaNO3	2419 μg h^{-1} cm^{-2}	92	[9]
Cu nanotubes	0.5 M K_2SO_4 + 50 mg L^{-1} NO_3^--N	778.6μg h^{-1} mg^{-1}	85.7	[10]

PdBP NAs	0.5 M K_2SO_4 + 100 mg L^{-1} KNO_3-N	0.11 mmol h^{-1} cm^{-2}	64.73	[11]
Pd/TiO_2	1 M LiCl + 0.25 M $LiNO_3$	0.066 mmol h^{-1} cm^{-2}	92.05	[12]

References

[1] Chen Q, Liang J, Liu Q, et al. Co nanoparticle-decorated pomelo-peel-derived carbon enabled high-efficiency electrocatalytic nitrate reduction to ammonia[J]. Chemical Communications, 2022, 58(26): 4259-4262.

[2] Zhao X, Geng Q, Dong F, et al. Boosting the selectivity and efficiency of nitrate reduction to ammonia with a single-atom Cu electrocatalyst[J]. Chemical Engineering Journal, 2023, 466: 143314.

[3] Wu Z Y, Karamad M, Yong X, et al. Electrochemical ammonia synthesis via nitrate reduction on Fe single atom catalyst[J]. Nature communications, 2021, 12(1): 2870.

[4] Tao W, Wang P, Li H, et al. Engineering sulfur vacancies optimization in $Ni_3Co_6S_8$ nanospheres toward extraordinarily efficient nitrate electroreduction to ammonia[J]. Applied Catalysis B: Environmental, 2023, 324: 122193.

[5] Hu J, Ma A, Wu X, et al. Mn_3O_4/CuOx heterostructure for nitrate electroreduction to ammonia[J]. Chemical Communications, 2023, 59(47): 7232-7235.

[6] Ye, S., Yang, X., Huang, Z. et al. The activity origin of FeCo Prussian blue analogue for ambient electrochemical hydrogenation of nitrate to ammonia in neutral electrolyte[J]. Science China Materials, 2023, 66, 3573–3581.

[7] Zhang S, Wu J, Zheng M, et al. Fe/Cu diatomic catalysts for electrochemical nitrate reduction to ammonia[J]. Nature Communications, 2023, 14(1): 3634.

[8] Zheng Y, Qin M X, Yu X, et al. Constructing Ru@C_3N_4/Cu tandem electrocatalyst with dual-active sites for enhanced nitrate electroreduction to ammonia[J]. Small, 2023: 2302266.

[9] Liu Q, Liu Q, Xie L, et al. High-performance electrochemical nitrate reduction to ammonia under ambient conditions using a FeOOH nanorod catalyst[J]. ACS Applied Materials & Interfaces, 2022, 14(15): 17312-17318.

[10] Li C, Liu S, Xu Y, et al. Controllable reconstruction of copper nanowires into nanotubes for efficient electrocatalytic nitrate conversion into ammonia[J]. Nanoscale, 2022, 14(34): 12332-12338.

[11] Xu Y, Sheng Y, Wang M, et al. Lattice-strain and Lewis acid sites synergistically promoted nitrate electroreduction to ammonia over PdBP nanothorn arrays[J]. Journal of Materials Chemistry A, 2022, 10(30): 16290-16296.

[12] Guo Y, Zhang R, Zhang S, et al. Pd doping-weakened intermediate adsorption to promote electrocatalytic nitrate reduction on TiO_2 nanoarrays for ammonia production and energy supply with zinc–nitrate batteries[J]. Energy & Environmental Science, 2021, 14(7): 3938-3944.